Minimal sensitivity optimisation of perturbatively approximated excited-state wavefunctions of the quartic oscillator

1986 J. Phys. A: Math. Gen. 19 3807

(http://iopscience.iop.org/0305-4470/19/18/026)

J. Phys. A: Math. Gen. 19 (1986) 3807-3821. Printed in Great Britain

Minimal sensitivity optimisation of perturbatively approximated excited-state wavefunctions of the quartic oscillator†

S K Kauffmann and S M Perez

Department of Physics, University of Cape Town, Rondebosch, Cape Province, 7700 Republic of South Africa

Received 28 January 1986

Abstract. The direct point-by-point application of minimal sensitivity optimisation to the first-order perturbative approximation to the ground-state wavefunction of the quartic oscillator, carried out previously, is extended to low-lying excited states. An analytic formula for the derivative with respect to the redundant parameter is developed and used to obtain the minimally sensitive value for this parameter as a function of configuration space. Generally, more than one such minimally sensitive value is found at each configuration space point—these values are categorised into disjoint continuous curves. For all the cases studied, it has proved possible to piece together sections of such curves in an unambiguous manner so as to obtain optimised wavefunction approximations which are both renormalisable and continuously differentiable. Comparison of these optimised wavefunction approximations with the exact results revealed satisfactory agreement, particularly in the large $|x|$ asymptotic region where orthodox perturbation methods fail completely due to the strong coupling.

1. Introduction

In a previous paper (Kauffmann and Perez 1984) we have outlined the direct optimisation of perturbative approximations to configuration space wavefunctions using Stevenson's principle of minimal sensitivity (PMS) (Stevenson 1981) and have applied this technique to the ground-state wavefunction of the quartic oscillator. The success of this new method in dealing with the ground-state wavefunction was encouraging, but a demonstration of its ability to decently approximate the excited-state wavefunctions as well would be even more persuasive. The algebraic manipulation used in optimising the perturbative ground state of the quartic oscillator rapidly becomes more laborious for the excited states as the principal quantum number increases. We have managed to overcome this by making use of the harmonic oscillator generating function and raising and lowering operators to deduce an analytic closed form for the derivative with respect to the redundant parameter of the first-order perturbative approximation to the quartic oscillator nth stationary-state wavefunction.

Having thus achieved the same degree of analytic progress for the nth stationary state as we previously had attained for only the ground state, we apply numerical minimum finding methods to locate, at each configuration space point x, the minimally

† Work supported in part by CSIR/FRD grant.

0305-4470/86/183807+15$02.50

sensitive value of the redundant parameter. Very frequently an ambiguity is encountered, where more than one such value exists at a given x. In the case of the ground state, we saw that only one of the possible minimally sensitive continuous dependences of the redundant parameter on x could yield a renormalisable wavefunction approximation. For the excited states it turns out that *none* of the possible minimally sensitive continuous dependences of the redundant parameter on x yields, by itself, a renormalisable wavefunction approximation. However, for all the excited states studied, it proved possible to unambiguously piece together sections of two or more such continuous dependences in such a way as to obtain a renormalisable and continuously differentiable wavefunction approximation.

The accuracy of these optimised approximations is quite acceptable, particularly in the large $|x|$ asymptotic region where unoptimised perturbation theory breaks down completely. The number of pieced together sections needed for the x-dependent redundant parameter increases with the principal quantum number of the excited state, making its graph increasingly jagged, although the corresponding wavefunction approximations are, of course, completely smooth (continuously differentiable).

In § 2 we briefly review the use of PMS for the optimisation of first-order perturbative approximations, including circumstances where this yields exact results, while in § 3 we present the analytic formulae required for the application of this method to the nth stationary-state wavefunction of the quartic oscillator. In § 4, numerical results, in both graphical and abbreviated tabular form, are given for the quartic oscillator ground state and lowest four excited states; the need for and method of piecing together sections of certain minimally sensitive continuous dependences of the redundant parameter on x is described and illustrated.

2. PMS optimisation of first-order perturbative approximations

PMS optimisation can be applied to choose between those perturbative approximations to a physical quantity which result from the different members of a parametrised class of unperturbed Hamiltonians. The exact value of the physical quantity under consideration depends only on the exact Hamiltonian; it is entirely independent of which unperturbed Hamiltonian is chosen to obtain its perturbative approximation. Thus it is independent of the value of the parameter which selects the member of the class of unperturbed Hamiltonians being considered. Normally, however, the perturbative approximation to the exact value can be expected to depend on the unperturbed Hamiltonian used, and thus on the value of the parameter which selects this unperturbed Hamiltonian. Appealing to the commonsense idea that approximations should be constructed so as to incorporate known properties of the exact result to the greatest extent possible (Stevenson 1981), we readily arrive at the prescription that the optimum value of the redundant parameter occurs where the corresponding perturbative approximations are least sensitive to small changes in it.

Let us denote the exact Hamiltonian of the physical system under discussion as H and the parametrised class of unperturbed Hamiltonians as $H_0(\boldsymbol{\lambda})$, where $\boldsymbol{\lambda} \equiv (\lambda_1, \lambda_2, .., \lambda_n)$ is a multidimensional (vector) parameter. We may write

$$H = H_0(\boldsymbol{\lambda}) + V(\boldsymbol{\lambda}) \tag{2.1a}$$

where, of course,

$$V(\boldsymbol{\lambda}) \equiv (H - H_0(\boldsymbol{\lambda})) \tag{2.1b}$$

and proceed to calculate perturbative approximations to a physical quantity—these consist of the sums of all the perturbative contributions through some given order in $V(\lambda)$. Such approximations can normally be expected to vary with λ, though the exact value of the physical quantity is completely insensitive to λ. PMS instructs us to choose the λ value for the optimum approximation as that one whose approximation is the least sensitive to small changes in λ.

An interesting special case, albeit one which cannot be practically exploited, occurs when there exists a particular value λ' of λ such that

$$H = H_0(\lambda'). \tag{2.2a}$$

In such a case

$$V(\lambda = \lambda') = 0 \tag{2.2b}$$

causing all *second- or higher-order* perturbative contributions (in $V(\lambda)$) to any physical quantity to be stationary in λ at $\lambda = \lambda'$. The sum of *all orders* of perturbative contributions in $V(\lambda)$ is, of course, the exact result for the value of the physical quantity, which we have seen to be constant in λ, i.e. stationary at all λ—in particular at $\lambda = \lambda'$. Thus the sum of the *zeroth- and first-order* perturbative contributions in $V(\lambda)$ to the physical quantity (namely its first-order perturbative approximation) must consequently be stationary in λ at $\lambda = \lambda'$. Thus if we perform PMS optimisation of a first-order perturbative approximation in this context to any physical quantity, we will find a minimally sensitive (stationary) value for λ at $\lambda = \lambda'$. At this value of λ, $V(\lambda)$ vanishes and $H_0(\lambda) = H$, causing the first-order perturbative approximation to become *exact.*

Thus, in the case where equation (2.2*a*) holds, PMS optimisation obtains the *exact* result already from *first-order perturbation theory* (and also, of course from any higher-order perturbative approximation). However, equation (2.2*a*) will not hold true in any practical case, for it implies that H is completely solvable, since $H_0(\lambda')$, an unperturbed Hamiltonian, is required to be so. Nonetheless, there is some insight to be gained from the above exercise—if $H_0(\lambda)$ well approximates H, at least for the physical quantity under investigation, for some value λ' of λ, then we may already expect PMS optimisation of *first-order* perturbation theory to yield a rather accurate result. It has, indeed, been observed that PMS optimisation often does give surprisingly good results from first-order perturbation theory (Stevenson 1981). We note that equation (2.2*a*) is a generalisation of the condition given in our previous paper (Kauffmann and Perez 1984), where we had required that $H_0(\lambda)$ be a linear form in λ.

3. Application of PMS to the configuration space stationary states of the quartic oscillator

The quartic oscillator is described by the exact Hamiltonian

$$H = \tfrac{1}{2}(p^2 + x^4) \tag{3.1a}$$

which we approximate by a parametrised class of unperturbed harmonic oscillator Hamiltonians

$$H_0(\lambda) = \tfrac{1}{2}(p^2 + \lambda^2 x^2) \tag{3.1b}$$

resulting in the perturbative potential

$$V(\lambda) = \tfrac{1}{2}(x^4 - \lambda^2 x^2). \tag{3.1c}$$

To carry out the first-order perturbation of the stationary states of $H_0(\lambda)$, it is convenient to express $V(\lambda)$ in terms of the harmonic oscillator stationary-state raising and lowering operators. These are

$$a \equiv (2\lambda)^{-1/2}(ip + \lambda x) \tag{3.2a}$$

and

$$a^+ \equiv (2\lambda)^{-1/2}(-ip + \lambda x). \tag{3.2b}$$

The unperturbed harmonic oscillator stationary-state wavefunctions, $\Psi_n^{(0)}(x;\lambda)$, $n = 0, 1, 2, \ldots$, which satisfy the energy eigenvalue equations

$$H_0(\lambda)\Psi_n^{(0)}(x;\lambda) = E_n^{(0)}(\lambda)\Psi_n^{(0)}(x;\lambda) \qquad E_n^{(0)}(\lambda) \equiv (n+\tfrac{1}{2})\lambda \qquad n = 0, 1, 2, \ldots \tag{3.3a}$$

are affected by a and a^+ according to the equations

$$a\Psi_n^{(0)}(x;\lambda) = n^{1/2}\Psi_{n-1}^{(0)}(x;\lambda) \tag{3.3b}$$

and

$$a^+\Psi_n^{(0)}(x;\lambda) = (n+1)^{1/2}\Psi_{n+1}^{(0)}(x;\lambda). \tag{3.3c}$$

The explicit form of the normalised unperturbed harmonic oscillator ground-state wavefunction is given by

$$\Psi_0^{(0)}(x;\lambda) = (\lambda/\pi)^{1/4}\exp(-\tfrac{1}{2}\lambda x^2) \tag{3.4a}$$

which, by repeated application of the raising operator a^+, can be made to yield the nth unperturbed harmonic oscillator excited-state wavefunction,

$$\Psi_n^{(0)}(x;\lambda) = (n!)^{-1/2}(a^+)^n\Psi_0^{(0)}(x;\lambda). \tag{3.4b}$$

Using equation (3.2) we can express the coordinate operator x in terms of a and a^+,

$$x = (2\lambda)^{-1/2}(a + a^+) \tag{3.5}$$

permitting us to re-express the perturbative potential $V(\lambda)$, equation (3.1c), in terms of a and a^+:

$$V(\lambda) = (8\lambda^2)^{-1}(a^4 + 2[(2a^+a+3) - \lambda^3]a^2 + \{3[2(a^+a)^2 + 2a^+a + 1] - 2\lambda^3(2a^+a+1)\} + 2(a^+)^2[(2a^+a+3) - \lambda^3] + (a^+)^4). \tag{3.6}$$

Thus, combining equations (3.6), (3.3b) and (3.3c) we find

$$\begin{aligned} V(\lambda)\Psi_n^{(0)}(x;\lambda) = (8\lambda^2)^{-1}\{&[n(n-1)(n-2)(n-3)]^{1/2}\Psi_{n-4}^{(0)}(x;\lambda) \\ &+ 2[(2n-1) - \lambda^3][n(n-1)]^{1/2}\Psi_{n-2}^{(0)}(x;\lambda) \\ &+ [3(2n^2+2n+1) - 2\lambda^3(2n+1)]\Psi_n^{(0)}(x;\lambda) \\ &+ 2[(2n+3) - \lambda^3][(n+1)(n+2)]^{1/2}\Psi_{n+2}^{(0)}(x;\lambda) \\ &+ [(n+1)(n+2)(n+3)(n+4)]^{1/2}\Psi_{n+4}^{(0)}(x;\lambda)\}. \end{aligned} \tag{3.7}$$

The unperturbed basis matrix elements of $V(\lambda)$, which may be read off from equation (3.7), enable us to write down the first-order perturbative approximations (sum of the zeroth- plus first-order contributions in $V(\lambda)$) to both the energy eigenvalues and the stationary-state wavefunctions of the quartic oscillator. The first-order perturbative approximation to the energy eigenvalues is

$$E_n^{(0,1)}(\lambda) = (n+\tfrac{1}{2})\lambda + (8\lambda^2)^{-1}[3(2n^2+2n+1) - 2\lambda^3(2n+1)] \tag{3.8}$$

which, of course, varies with the value of the 'redundant' parameter λ. We invoke PMS to make an optimal choice of λ, namely that value of λ for which $E_n^{(0,1)}(\lambda)$ is minimally sensitive to small changes in λ,

$$\partial E_n^{(0,1)}(\lambda)/\partial\lambda = \tfrac{1}{4}[(2n+1) - 3(2n^2+2n+1)\lambda^{-3}] = 0. \tag{3.9a}$$

This results in the energy-optimised value of λ, which we note depends on the principal quantum number n, to be

$$\lambda_n = [3(2n^2+2n+1)/(2n+1)]^{1/3} \tag{3.9b}$$

resulting in the PMS-optimised first-order perturbative approximation to the energy eigenvalues (Stevenson 1981)

$$E_n^{(0,1)}(\lambda_n) = \tfrac{3}{8}[3(2n^2+2n+1)(2n+1)^2]^{1/3} \qquad n = 0, 1, 2, \ldots . \tag{3.9c}$$

It has been noted (Stevenson 1981) that equation (3.9c) is never in error by more than 2% for the energy eigenvalue spectrum of the quartic oscillator.

Similarly, we use the unperturbed matrix elements of $V(\lambda)$, as read off from equation (3.7), to obtain the first-order perturbative approximation to the stationary-state wavefunctions of the quartic oscillator

$$\begin{aligned}\Psi_n^{(0,1)}(x;\lambda) = \Psi_n^{(0)}(x;\lambda) &+ (32\lambda^3)^{-1}\{[n(n-1)(n-2)(n-3)]^{1/2}\Psi_{n-4}^{(0)}(x;\lambda) \\ &+ 4[(2n-1)-\lambda^3][n(n-1)]^{1/2}\Psi_{n-2}^{(0)}(x;\lambda) \\ &+ 4[\lambda^3-(2n+3)][(n+1)(n+2)]^{1/2}\Psi_{n+2}^{(0)}(x;\lambda) \\ &- [(n+1)(n+2)(n+3)(n+4)]^{1/2}\Psi_{n+4}^{(0)}(x;\lambda)\}. \end{aligned} \tag{3.10}$$

In order to be able to find the PMS-optimised value of the 'redundant' parameter λ in equation (3.10), we require $\partial\Psi_n^{(0,1)}(x;\lambda)/\partial\lambda$, and thus $\partial\Psi_m^{(0)}(x;\lambda)/\partial\lambda$ for any $m = 0, 1, 2, \ldots$. Unfortunately, the algebraic dependence of $\Psi_m^{(0)}(x;\lambda)$ on λ rapidly becomes more complicated as m increases. We can, however, sidestep this algebraic complexity by working with the generating function for the $\Psi_m^{(0)}(x;\lambda)$, defined as

$$G^{(0)}(x;s;\lambda) \equiv \sum_{m=0}^{\infty} s^m (m!)^{-1/2}\Psi_m^{(0)}(x;\lambda) \tag{3.11a}$$

which may be re-expressed as

$$G^{(0)}(x;s;\lambda) = \sum_{m=0}^{\infty} s^m (m!)^{-1}(a^+)^m\Psi_0^{(0)}(x;\lambda) = \exp(sa^+)\Psi_0^{(0)}(x;\lambda) \tag{3.11b}$$

with an explicit representation

$$G^{(0)}(x;s;\lambda) = (\lambda/\pi)^{1/4}\exp[-\tfrac{1}{2}\lambda x^2 + (2\lambda)^{1/2}xs - \tfrac{1}{2}s^2]. \tag{3.11c}$$

Equation (3.11c) may now be differentiated with respect to λ to yield

$$\partial G^{(0)}(x;s;\lambda)/\partial\lambda = (4\lambda)^{-1}(1 - 2\lambda x^2 + 2(2\lambda)^{1/2}xs)G^{(0)}(x;s;\lambda). \tag{3.12}$$

To make further progress, the factor on the right-hand side of equation (3.12) which multiplies $G^{(0)}(x;s;\lambda)$ needs to be re-expressed in terms of a and a^+ instead of x and s. This is done by noting that

$$sG^{(0)}(x;s;\lambda) = aG^{(0)}(x;s;\lambda). \tag{3.13}$$

Equation (3.13), together with equation (3.5) for x, permits us to partially substitute for x and s in favour of a and a^+ in equation (3.12). A little algebra yields the result

$$\partial G^{(0)}(x; s; \lambda)/\partial\lambda = (4\lambda)^{-1}(a^2-(a^+)^2)G^{(0)}(x; s; \lambda) \tag{3.14}$$

which implies, from the definition (3.11a) of $G^{(0)}(x; s; \lambda)$ and the fact that the operators a, a^+ and $\partial/\partial\lambda$ all commute with the quantity s, that

$$\partial\Psi_m^{(0)}(x; \lambda)/\partial\lambda = (4\lambda)^{-1}(a^2-(a^+)^2)\Psi_m^{(0)}(x; \lambda) \qquad m = 0, 1, 2, \ldots \tag{3.15a}$$

or, using the lowering and raising properties of a and a^+,

$$\partial\Psi_m^{(0)}(x; \lambda)/\partial\lambda = (4\lambda)^{-1}\{[m(m-1)]^{1/2}\Psi_{m-2}^{(0)}(x; \lambda) - [(m+1)(m+2)]^{1/2}\Psi_{m+2}^{(0)}(x; \lambda)\}. \tag{3.15b}$$

Equation (3.15b) allows us at last to realise our goal of differentiating the first-order perturbative approximation to the quartic oscillator stationary-state wavefunctions, equation (3.10), with respect to the 'redundant' parameter λ:

$$\begin{aligned}
\partial\Psi_n^{(0,1)}(x; \lambda)/\partial\lambda &= (128\lambda^4)^{-1}\{[n(n-1)(n-2)(n-3)(n-4)(n-5)]^{1/2}\Psi_{n-6}^{(0)}(x; \lambda) \\
&\quad + 4[2(n-2)-\lambda^3][n(n-1)(n-2)(n-3)]^{1/2}\Psi_{n-4}^{(0)}(x; \lambda) \\
&\quad + [32\lambda^3-(n^2+91n-42)][n(n-1)]^{1/2}\Psi_{n-2}^{(0)}(x; \lambda) \\
&\quad + 8[(n^2+n+1)\lambda^3-(2n^3+3n^2+7n+3)]\Psi_n^{(0)}(x; \lambda) \\
&\quad - [32\lambda^3+(n^2-89n-132)][(n+1)(n+2)]^{1/2}\Psi_{n+2}^{(0)}(x; \lambda) \\
&\quad + 4[2(n+3)-\lambda^3][(n+1)(n+2)(n+3)(n+4)]^{1/2}\Psi_{n+4}^{(0)}(x; \lambda) \\
&\quad + [(n+1)(n+2)(n+3)(n+4)(n+5)(n+6)]^{1/2}\Psi_{n+6}^{(0)}(x; \lambda)\}.
\end{aligned} \tag{3.16}$$

With equations (3.10) and (3.16) we have achieved the same degree of analytic progress in applying PMS optimisation to the first-order perturbative approximation to the quartic oscillator nth stationary-state wavefunction as had been previously attained (Kauffmann and Perez 1984) for only the ground-state wavefunction. The remaining work to be done is essentially numerical in nature—at each value of x a search is to be made for that value of λ which will minimise the 'sensitivity measure' $(\partial\Psi_n^{(0,1)}(x; \lambda)/\partial\lambda)^2$ of the dependence of $\Psi_n^{(0,1)}(x; \lambda)$ on λ. This is done in small increments of x, with the previously determined minimally sensitive value for λ used to begin the search procedure at the incremented x, thus ensuring a continuous dependence of the resulting 'optimal' $\lambda_n(x)$ on x. Except for an occasional short interval in x, it is found, in practice, that this procedure locates stationary values of λ, i.e. those which satisfy $\partial\Psi_n^{(0,1)}(x; \lambda)/\partial\lambda = 0$. The advantage of the minimisation procedure adopted over searching for stationary λ values is that it avoids gaps in $\lambda_n(x)$ in those short x intervals where the stationary condition cannot be satisfied with a continuous $\lambda_n(x)$ (Kauffmann and Perez 1984). Finally, the continuous $\lambda_n(x)$ thus found is to be substituted into $\Psi_n^{(0,1)}(x; \lambda)$ to obtain the PMS-optimised first-order perturbative approximation $\Psi_n^{(0,1)}(x; \lambda_n(x))$ which must finally be renormalised, as is generally true of perturbative wavefunction approximations.

Before embarking on the numerical programme outlined above, a few loose ends need to be tied up analytically. First we require an efficient procedure for numerically generating the unperturbed harmonic oscillator stationary-state wavefunctions $\Psi_m^{(0)}(x; \lambda)$ which occur in such profusion in the key formulae (3.10) and (3.16). We

can obtain a recurrence relation by multiplying $\Psi_m^{(0)}(x;\lambda)$ by $(2\lambda)^{1/2}x$ which, from equation (3.5), is equal to $(a+a^+)$. Using the lowering and raising properties of a and a^+ we obtain

$$\Psi_{m+1}^{(0)}(x;\lambda)=[2\lambda/(m+1)]^{1/2}x\Psi_m^{(0)}(x;\lambda)-[m/(m+1)]^{1/2}\Psi_{m-1}^{(0)}(x;\lambda). \tag{3.17}$$

This, combined with the explicit form (3.4a) for $\Psi_0^{(0)}(x;\lambda)$ allows all the $\Psi_m^{(0)}(x;\lambda)$ to be numerically generated. In particular we can obtain

$$\Psi_1^{(0)}(x;\lambda)=(2\lambda)^{1/2}x\Psi_0^{(0)}(x;\lambda) \tag{3.18}$$

and, for $|x|\to\infty$, the asymptotic behaviour

$$\Psi_m^{(0)}(x;\lambda)\sim(m!)^{-1/2}[(2\lambda)^{1/2}x]^m\Psi_0^{(0)}(x;\lambda). \tag{3.19}$$

Since the $\Psi_m^{(0)}(x;\lambda)$ which occur in equations (3.10) and (3.16) all have m values which differ from each other by a multiple of two, it is even more efficient to use a recurrence relation which increments m in steps of two. This can be generated by multiplying $\Psi_m^{(0)}(x;\lambda)$ by $2\lambda x^2$, which is equal to $(a+a^+)^2$. The resulting recurrence relation is

$$\begin{aligned}\Psi_{m+2}^{(0)}(x;\lambda)=&[(m+2)(m+1)]^{-1/2}\{(2\lambda x^2-2m-1)\Psi_m^{(0)}(x;\lambda)\\&-[m(m-1)]^{1/2}\Psi_{m-2}^{(0)}(x;\lambda)\}\end{aligned} \tag{3.20}$$

which must be used in conjunction with the explicit forms of $\Psi_0^{(0)}(x;\lambda)$ or $\Psi_1^{(0)}(x;\lambda)$ given in equations (3.4a) and (3.18) to generate all the even m or odd m wavefunctions $\Psi_m^{(0)}(x;\lambda)$.

Finally, to aid the numerical tracing out of the minimally sensitive continuous $\lambda_n(x)$, it is useful to be able to begin from analytically determinable optimal λ values which may be calculable at certain special values of x. For example, at $x=0$ we can use the forms (3.11a) and (3.11c) of the generating function to obtain

$$\begin{Bmatrix}\Psi_{2k}^{(0)}(x=0;\lambda)\\ \Psi_{2k+1}^{(0)}(x=0;\lambda)\end{Bmatrix}=\begin{Bmatrix}(\lambda/\pi)^{1/4}(-\tfrac{1}{2})^k[(2k)!]^{1/2}(k!)^{-1}\\ 0\end{Bmatrix}\qquad k=0,1,2,\ldots \tag{3.21}$$

which can be inserted into equation (3.16) to obtain

$$\begin{Bmatrix}\partial\Psi_{2l}^{(0,1)}(x=0;\lambda)/\partial\lambda\\ \partial\Psi_{2l+1}^{(0,1)}(x=0;\lambda)/\partial\lambda\end{Bmatrix}=\begin{Bmatrix}(\lambda/\pi)^{1/4}(-\tfrac{1}{2})^l[(2l)!]^{1/2}(128\lambda^4 l!)^{-1}[28\lambda^3-99(4l+1)]\\ 0\end{Bmatrix}$$

$$l=0,1,2,\ldots. \tag{3.22}$$

Thus, for odd n, $\Psi_n^{(0,1)}(x=0;\lambda)$ is stationary for *all* values of λ (indeed it is equal to zero for all λ), while for even $n=2l$, the only finite, real stationary value occurs at

$$\lambda_{2l}(x=0)=[99(4l+1)/28]^{1/3}\qquad l=0,1,2,\ldots \tag{3.23}$$

which provides a convenient starting value for the numerical tracing out of the continuous $\lambda_{2l}(x)$, $l=0,1,2,\ldots$.

It also proves to be possible to analytically determine the asymptotic behaviour of $\lambda_n(x)$ as $|x|\to\infty$. In the limit $x\to+\infty$ it can be shown from Schrödinger's equation that the exact stationary-state wavefunctions of the quartic oscillator all have the asymptotic behaviour (not normalised)

$$\Psi_n(x)\sim x^{-1}\exp(-x^3/3)\qquad\text{as } x\to+\infty. \tag{3.24}$$

Given the dominant exponential behaviour imposed by the factor $\exp(-\frac{1}{2}\lambda x^2)$ on $\Psi_n^{(0,1)}(x;\lambda)$ as $|x|\to\infty$, the asymptotic behaviour (3.24) of the exact $\Psi_n(x)$ suggests that the asymptotic behaviour of λ_n should be of the form

$$\lambda_n(x)\sim c|x| \qquad \text{as } |x|\to\infty \tag{3.25}$$

where c is a positive constant independent of $|x|$ and n, with a value in the vicinity of $\frac{2}{3}$. If we bear in mind the ansatz (3.25) while inserting the asymptotic form (3.19) of $\Psi_m^{(0)}(x;\lambda)$ into the formula (3.16) for $\partial\Psi_n^{(0,1)}(x;\lambda)/\partial\lambda$, we arrive at the following result for its asymptotic behaviour:

$$\partial\Psi_n^{(0,1)}(x;\lambda)/\partial\lambda\sim(\lambda/\pi)^{1/4}[(2\lambda)^{1/4}x]^{n+6}[128\lambda^4(n!)^{1/2}]^{-1}$$
$$\times[1-2(\lambda/x)^2]\exp(-\tfrac{1}{2}\lambda x^2) \qquad \text{as } |x|\to\infty \tag{3.26}$$

which implies that the asymptotic behaviour of the stationary value of λ is

$$\lambda_n(x)\sim 2^{-1/2}|x| \qquad \text{as } |x|\to\infty \tag{3.27}$$

consistent with the ansatz (3.25) for $c=2^{-1/2}$, which is slightly larger than $\frac{2}{3}$. Equation (3.27) provides a convenient approximate starting value of λ (at some $|x|\gg 1$) for the numerical tracing out of the minimally sensitive continuous $\lambda_n(x)$ curve, just as equation (3.23) provides such a starting value.

For the ground state, $n=0$, we have previously seen that the solution (3.23) having $\lambda_0(x=0)=(99/28)^{1/3}$ does indeed proceed continuously towards the asymptotic form (3.27), $\lambda_0(x)\sim 2^{-1/2}|x|$, as $|x|\to\infty$ (Kauffmann and Perez 1984). In the next section we shall see that matters do not work out quite so straightforwardly for the excited states, which require a piecing together of sections from more than just one minimally sensitive continuous $\lambda_n(x)$ curve.

4. PMS-optimised first-order perturbative results for the first five quartic oscillator stationary-state wavefunctions

For all the quartic oscillator *excited*-state first-order perturbative wavefunction approximations studied, the attempt to trace a continuous optimum $\lambda_n(x)$, $n\geq 1$, from its asymptotic behaviour $2^{-1/2}|x|$ at large $|x|$, equation (3.27), leads to an unacceptable divergence in its value toward $+\infty$ for $|x|$ tending toward zero. We can see this behaviour clearly in figure 1(*a*) depicted in the outermost (broken) curve for $\lambda_4(x)$. It is unacceptable because its substitution into $\Psi_n^{(0,1)}(x;\lambda)$, equation (3.10), to produce the PMS-optimised $\Psi_n^{(0,1)}(x;\lambda_n(x))$, results in the latter's divergence as $|x|\to\infty$ as well, rendering it unrenormalisable and thus unphysical. This behaviour of $\Psi_4^{(0,1)}(x;\lambda_4(x))$ is shown in figure 1(*b*), also in the outermost (broken) curve. Only in the ground-state, $n=0$, case previously studied (Kauffmann and Perez 1984) does the correct $2^{-1/2}|x|$ large $|x|$ behaviour of $\lambda_n(x)$ connect continuously to a sensible finite value as $|x|\to 0$.

Nonetheless, we have seen from equations (3.22) and (3.23) that for all even values of n, there does exist a unique sensible (i.e. finite and positive) stationary value for $\lambda_n(x)$ as $|x|\to 0$. This is also the case for the two odd n values we have studied numerically (for odd n, *all* λ values are stationary *at* $x=0$, but we do get *unique* finite and positive values for $\lambda_n(x)$ in the *limit* $|x|\to 0$, at least for the odd n values 1 and 3 we have studied). If we start with these unique acceptable stationary values for $\lambda_n(x)$ as $|x|\to 0$ and continuously trace the resulting optimised $\lambda_n(x)$ curves toward

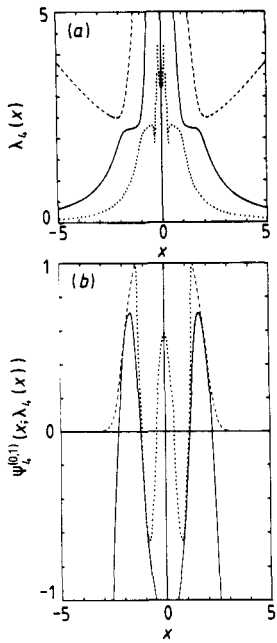

Figure 1. (*a*) Three minimally sensitive continuous positive curves for $\lambda_4(x)$. The dotted curve leads to physically sensible behaviour of the corresponding optimised wavefunction approximation for $|x|$ values sufficiently close to zero, the broken curve does the same for all sufficiently large $|x|$, while the full curve does this for the remaining intermediate $|x|$. (*b*) The three corresponding minimally sensitive wavefunction approximations $\Psi_4^{(0,1)}(x;\lambda_4(x))$. Note how the intermediate full curve closely parallels the dotted curve for $|x| \simeq 0.96$ and does the same to the broken curve for $|x| \simeq 1.85$.

larger values of $|x|$, we find that, with the sole exception of $n = 0$, they fail to coincide with the continuous $\lambda_n(x)$ curves traced inward from the asymptotic behaviour $2^{-1/2}|x|$ at large $|x|$. Indeed, for the excited states, the small $|x|$ sensible $\lambda_n(x)$ curves all tend toward zero for large $|x|$. This causes the resulting $\Psi_n^{(0,1)}(x;\lambda_n(x))$ to diverge as $|x| \to \infty$, making it unrenormalisable and thus unphysical at large $|x|$. We can see this behaviour in the innermost (dotted) curves for $\lambda_4(x)$ and $\Psi_4^{(0,1)}(x;\lambda_4(x))$ in figures 1(*a*) and 1(*b*).

For the excited states, we thus see that the continuous $\lambda_n(x)$ which causes $\Psi_n^{(0,1)}(x;\lambda_n(x))$ to behave sensibly (so that it might be renormalisable) as $|x| \to 0$ causes it to behave unphysically (so that it is unrenormalisable) as $|x| \to \infty$. A second continuous $\lambda_n(x)$, lying entirely above this one, has just the reverse attributes. However, it turns out that for $n = 1$, 2 and 3, there is a region in $|x|$ where the two corresponding $\Psi_n^{(0,1)}(x;\lambda_n))$ curves approach each other very closely and run nearly parallel. For $n = 4$ there is the additional complication in that a *third* continuous $\lambda_4(x)$ curve, lying *between* the two described above, is found—see the middle (full) curve in figure 1(*a*)—and it is the $\Psi_4^{(0,1)}(x;\lambda_4(x))$ corresponding to this third curve which closely approaches and parallels those corresponding to each of the first two curves in two separate regions of $|x|$. This behaviour is shown in figure 1(*b*), where this third $\Psi_4^{(0,1)}(x;\lambda_4(x))$ curve is the middle (full) one, which closely approaches and parallels the innermost (dotted) curve for $|x| \simeq 0.96$ and the outermost (broken) curve for $|x| \simeq 1.85$. We notice that this third curve has unphysical behaviour (not permitting

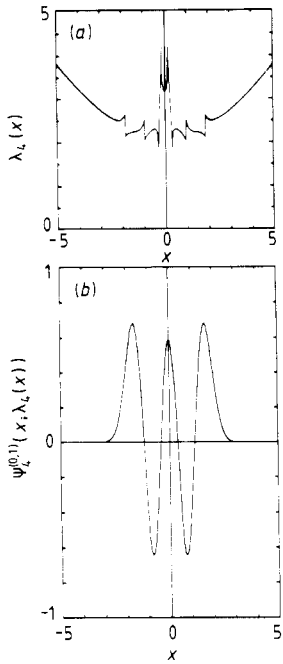

Figure 2. (*a*) Optimum $\lambda_4(x)$ curve, pieced together from sections of the three minimally sensitive $\lambda_4(x)$ curves of figure 1(*a*), showing jump discontinuities at $|x| \simeq 0.96$ and $|x| \simeq 1.85$, where their corresponding wavefunction approximations have matching logarithmic derivatives. (*b*) The corresponding smoothly pieced together optimum wavefunction approximation $\Psi_4^{(0,1)}(x; \lambda_4(x))$, which still requires an overall renormalisation factor.

renormalisation) *both* for $|x| \to 0$ and $|x| \to \infty$. For higher values of n it seems very likely that there will be even more continuous $\lambda_n(x)$ curves lying between the lowest (innermost) and highest (outermost) ones, with such adjacent $\lambda_n(x)$ curves having their corresponding $\Psi_n^{(0,1)}(x; \lambda_n(x))$ curves approach each other closely and nearly in parallel at particular $|x|$ values.

Near these $|x|$ values there is no basis on which to discriminate between the two pertinent competing $\Psi_n^{(0,1)}(x; \lambda_n(x))$ curves (Stevenson 1981), so it is permissible to switch from a $\lambda_n(x)$ curve which will soon cause $\Psi_n^{(0,1)}(x; \lambda_n(x))$ to take on unphysical values to one which will keep $\Psi_n^{(0,1)}(x; \lambda_n(x))$ in a physical regime over a longer $|x|$ domain. Before this $|x|$ domain is exhausted in turn, it is required that the close, nearly parallel $\Psi_n^{(0,1)}(x; \lambda_n(x))$ approach ambiguity will recur at a timely value of $|x|$, allowing a further $\lambda_n(x)$ curve switch, etc. The precise mechanics of the switch from one continuous $\lambda_n(x)$ curve to the next, and from its corresponding $\Psi_n^{(0,1)}(x; \lambda_n(x))$ curve to the next, is subjected to the physically sensible constraint that the resulting approximate wavefunction must be continuously differentiable. This condition is readily fulfilled in practice via the observation that $\Psi_n^{(0,1)}(x; \lambda_n(x))$ approximations involving distinct $\lambda_n(x)$ curves should generally require distinct renormalisation constants. We go to the $|x|$ value where the two nearly parallel $\Psi_n^{(0,1)}(x; \lambda_n(x))$ curves approach each other most closely. We search to either side of this $|x|$ value for the nearest $|x|$ where the logarithmic derivatives of the two $\Psi_n^{(0,1)}(x; \lambda_n(x))$ curves are equal. In practice, we have always found that the region of nearly parallel, closest approach of the two curves includes a point $|x|$ where their logarithmic derivatives

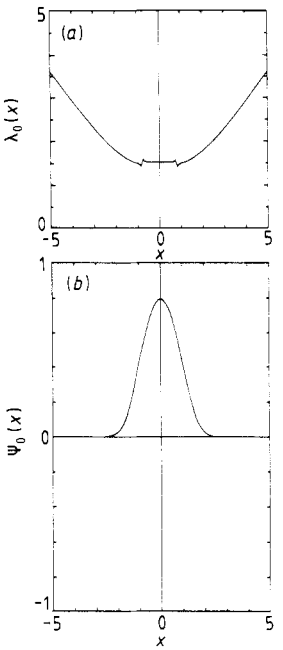

Figure 3. (*a*) Optimum $\lambda_0(x)$ curve. (*b*) The corresponding renormalised optimum wavefunction approximation $\Psi_0^{(0,1)}(x; \lambda_0(x))$ (dotted curve) together with the exact wavefunction $\Psi_0(x)$ (full curve). The dotted optimum approximation curve cannot be resolved.

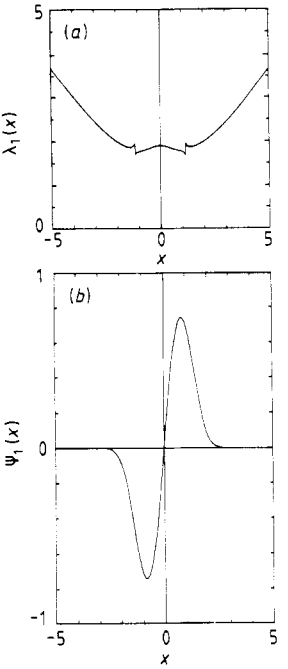

Figure 4. The same as figure 3 for the first excited state. The dotted optimum approximation curve cannot be resolved.

are equal. At this $|x|$ value we make the switch from the physically less propitious $\lambda_n(x)$ (for subsequent $|x|$ values) to the physically more propitious one, simultaneously multiplying one of the corresponding $\Psi_n^{(0,1)}(x; \lambda_n(x))$ curves by a relative renormalisation constant, chosen so that this curve is made equal to the other $\Psi_n^{(0,1)}(x; \lambda_n(x))$ curve at this $|x|$ value.

Thus, though the switch from one continuous $\lambda_n(x)$ to another generally involves a jump discontinuity, the join between their corresponding relatively renormalised $\Psi_n^{(0,1)}(x; \lambda_n(x))$ curve sections is completely smooth (continuously differentiable). For the case $n = 4$ we can observe the behaviour of these pieced together curves in figure 2. Figure 2(*a*) shows the pieced together $\lambda_4(x)$ curve, built from sections of the three $\lambda_4(x)$ curves shown in figure 1(*a*), having switched from one to the next at the two jump discontinuities at $|x| \simeq 0.96$ and $|x| \simeq 1.85$, where the logarithmic derivatives of the corresponding $\Psi_4^{(0,1)}(x; \lambda_4(x))$ are equal. On the other hand, the pieced together $\Psi_4^{0,1)}(x; \lambda_4(x))$ curve shown in figure 2(*b*) is completely smooth, for the sections of the three curves from figure 1(*b*) which comprise it are relatively renormalised to be equal at the switchover points, which in turn are located where the logarithmic derivatives of the pieced together curves match. The resulting smoothly pieced together wavefunction approximation curve will still require an overall renormalisation. It is worthwhile pointing out here that in all the cases studied, both the relative and overall renormalisation constants needed have come out quite close to unity, a partial testimony to the inherent trustworthiness of the approach.

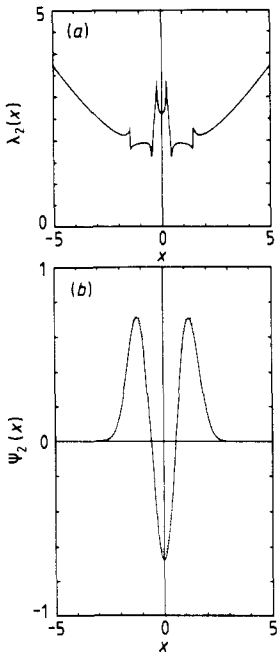

Figure 5. The same as figure 3 for the second excited state.

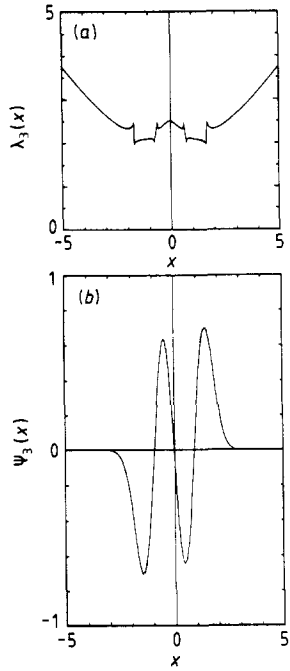

Figure 6. The same as figure 3 for the third excited state.

In addition to the jump discontinuities of the optimum $\lambda_4(x)$ curve shown in figure 2(a), we observe further cusps at $|x| \simeq 0.14$ and $|x| \simeq 0.33$. These are not due to discontinuities, but are already present in the innermost (dotted) continuous $\lambda_4(x)$ curve shown in figure 1(a). They are associated with the fact that this continuous $\lambda_4(x)$ curve does not consist of stationary values of $\Psi_4^{(0,1)}(x; \lambda)$ for $0.14 \leqslant |x| \leqslant 0.33$; it only locally minimises $(\partial \Psi_4^{(0,1)}(x; \lambda)/\partial \lambda)^2$ to non-zero values in this $|x|$ domain, which we may call a stationary λ value gap. For all other values of $|x|$, this $\lambda_4(x)$ consists entirely of stationary points and the other two continuous $\lambda_4(x)$ curves shown in figure 1(a) are both made up of only stationary λ values for all $|x|$. The existence of such cusps, apparently reflecting a discontinous derivative near the endpoints of a stationary λ value gap, has already been encountered for $n = 0$ (Kauffmann and Perez 1984) and we encounter it as well for $n = 2$ and 3. At the locations of these cusps the corresponding $\Psi_n^{(0,1)}(x; \lambda_n(x))$ curves are completely smooth and generally monotonic (for example, see the dotted curve in figure 1(b) for the case $n = 4$). Thus these cusp features at the endpoints of a stationary λ value gap pose no problems for the smoothness and physical acceptability of the corresponding $\Psi_n^{(0,1)}(x; \lambda_n(x))$ curves. Nonetheless it is of interest that the total number of cusps which are present on a pieced together $\lambda_n(x)$ curve, whether these are associated with gaps in stationary λ values or with jump discontinuities where curve sections are pieced together, seems to bear a simple relationship to n. An examination of figures 3(a)-7(a) shows that $\lambda_0(x)$ through to $\lambda_4(x)$ are consistent with the guess that the optimum $\lambda_{2n}(x)$ and $\lambda_{2n+1}(x)$ both have $4(n+1)$ cusps, $n = 0, 1, 2, \ldots$.

Finally, we wish to compare the optimised $\Psi_n^{(0,1)}(x; \lambda_n(x))$, after overall renormalisation, with the exact quartic oscillator stationary-state wavefunctions $\Psi_n(x)$, which

Table 1. Quartic oscillator ground-state wavefunction.

x	Point-by-point optimised $\lambda_0(x)$	Renormalised $\Psi_0^{(0,1)}(x;\lambda_0(x))$	Exact wavefunction $\Psi_0(x)$	Energy optimised λ_0	$\Psi_0^{(0)}(x;\lambda_0)$	Renormalised $\Psi_0^{(0,1)}(x;\lambda_0)$
0	1.52	0.795	0.793	1.44	0.823	0.796
0.5	1.52	0.692	0.691	1.44	0.687	0.692
1.0	1.50	0.425	0.427	1.44	0.400	0.425
1.5	1.60	0.156	0.159	1.44	0.162	0.152
2.0	1.78	2.73×10^{-2}	2.84×10^{-2}	1.44	4.60×10^{-2}	1.39×10^{-2}
2.5	2.02	1.74×10^{-3}	1.90×10^{-3}	1.44	9.08×10^{-3}	-1.17×10^{-2}
3.0	2.31	3.05×10^{-5}	3.72×10^{-5}	1.44	1.25×10^{-3}	-5.53×10^{-3}
3.5	2.61	1.11×10^{-7}	1.65×10^{-7}	1.44	1.20×10^{-4}	-1.18×10^{-3}
4.0	2.94	6.40×10^{-11}	1.29×10^{-10}	1.44	8.03×10^{-6}	-1.47×10^{-4}
4.5	3.27	4.44×10^{-15}	1.38×10^{-14}	1.44	3.75×10^{-7}	-1.16×10^{-5}
5.0	3.60	2.83×10^{-20}	1.57×10^{-19}	1.44	1.22×10^{-8}	-5.93×10^{-7}

Table 2. Quartic oscillator first excited-state wavefunction.

x	Point-by-point optimised $\lambda_1(x)$	Renormalised $\Psi_1^{(0,1)}(x;\lambda_1(x))$	Exact wavefunction $\Psi_1(x)$	Energy optimised λ_1	$\Psi_1^{(0)}(x;\lambda_1)$	Renormalised $\Psi_1^{(0,1)}(x;\lambda_1)$
0	1.89	0	0	1.71	0	0
0.5	1.83	0.609	0.608	1.71	0.641	0.611
1.0	1.75	0.705	0.704	1.71	0.676	0.706
1.5	1.87	0.356	0.359	1.71	0.348	0.353
2.0	1.99	7.65×10^{-2}	7.72×10^{-2}	1.71	0.104	6.13×10^{-2}
2.5	2.19	5.76×10^{-3}	5.85×10^{-3}	1.71	1.90×10^{-2}	-1.16×10^{-2}
3.0	2.44	1.18×10^{-4}	1.25×10^{-4}	1.71	2.17×10^{-3}	-6.69×10^{-3}
3.5	2.72	4.98×10^{-7}	5.89×10^{-7}	1.71	1.57×10^{-4}	-1.17×10^{-3}
4.0	3.02	3.31×10^{-10}	4.82×10^{-10}	1.71	7.28×10^{-6}	-1.04×10^{-4}
4.5	3.34	2.64×10^{-14}	5.35×10^{-14}	1.71	2.16×10^{-7}	-5.34×10^{-6}
5.0	3.66	1.92×10^{-19}	6.27×10^{-19}	1.71	4.14×10^{-9}	-1.63×10^{-7}

Table 3. Quartic oscillator second excited-state wavefunction.

x	Point-by-point optimised $\lambda_2(x)$	Renormalised $\Psi_2^{(0,1)}(x;\lambda_2(x))$	Exact wavefunction $\Psi_2(x)$	Energy optimised λ_2	$\Psi_2^{(0)}(x;\lambda_2)$	Renormalised $\Psi_2^{(0,1)}(x;\lambda_2)$
0	2.61	−0.645	−0.679	1.98	−0.630	−0.659
0.5	1.77	−0.127	−0.139	1.98	-4.13×10^{-3}	−0.122
1.0	1.92	0.652	0.630	1.98	0.694	0.646
1.5	2.22	0.572	0.572	1.98	0.536	0.572
2.0	2.16	0.161	0.163	1.98	0.177	0.155
2.5	2.33	1.46×10^{-2}	1.46×10^{-2}	1.98	3.05×10^{-2}	1.44×10^{-3}
3.0	2.55	3.47×10^{-4}	3.51×10^{-4}	1.98	2.91×10^{-3}	-5.31×10^{-3}
3.5	2.81	1.68×10^{-6}	1.80×10^{-6}	1.98	1.59×10^{-4}	-8.36×10^{-4}
4.0	3.10	1.27×10^{-9}	1.57×10^{-9}	1.98	5.07×10^{-6}	-5.50×10^{-5}
4.5	3.40	1.15×10^{-13}	1.83×10^{-13}	1.98	9.51×10^{-8}	-1.84×10^{-6}
5.0	3.72	9.49×10^{-19}	2.24×10^{-18}	1.98	1.06×10^{-9}	-3.33×10^{-8}

Table 4. Quartic oscillator third excited-state wavefunction.

x	Point-by-point optimised $\lambda_3(x)$	Renormalised $\Psi_3^{(0,1)}(x;\lambda_3(x))$	Exact wavefunction $\Psi_3(x)$	Energy optimised λ_3	$\Psi_3^{(0)}(x;\lambda_3)$	Renormalised $\Psi_3^{(0,1)}(x;\lambda_3)$
0	2.51	0	0	2.20	0	0
0.5	2.33	−0.634	−0.636	2.20	−0.565	−0.629
1.0	2.10	0.180	0.163	2.20	0.367	0.182
1.5	2.05	0.700	0.695	2.20	0.682	0.700
2.0	2.33	0.281	0.290	2.20	0.279	0.284
2.5	2.45	3.14×10^{-2}	3.22×10^{-2}	2.20	4.91×10^{-2}	2.25×10^{-2}
3.0	2.65	8.71×10^{-4}	8.84×10^{-4}	2.20	4.24×10^{-3}	-4.25×10^{-3}
3.5	2.90	4.83×10^{-6}	5.01×10^{-6}	2.20	1.91×10^{-4}	-7.31×10^{-4}
4.0	3.17	4.15×10^{-9}	4.71×10^{-9}	2.20	4.64×10^{-6}	-3.96×10^{-5}
4.5	3.46	4.22×10^{-13}	5.82×10^{-13}	2.20	6.16×10^{-8}	-9.71×10^{-7}
5.0	3.77	3.90×10^{-18}	7.43×10^{-18}	2.20	4.53×10^{-10}	-1.19×10^{-8}

Table 5. Quartic oscillator fourth excited-state wavefunction.

x	Point-by-point optimised $\lambda_4(x)$	Renormalised $\Psi_4^{(0,1)}(x;\lambda_4(x))$	Exact wavefunction $\Psi_4(x)$	Energy optimised λ_4	$\Psi_4^{(0)}(x;\lambda_4)$	Renormalised $\Psi_4^{(0,1)}(x;\lambda_4)$
0	3.17	0.591	0.616	2.39	0.572	0.586
0.5	2.30	−0.290	−0.265	2.39	−0.388	−0.279
1.0	2.46	−0.404	−0.401	2.39	−0.163	−0.400
1.5	2.23	0.618	0.614	2.39	0.702	0.628
2.0	2.51	0.423	0.446	2.39	0.406	0.437
2.5	2.56	6.03×10^{-2}	6.36×10^{-2}	2.39	7.78×10^{-2}	5.63×10^{-2}
3.0	2.75	1.98×10^{-3}	2.05×10^{-3}	2.39	6.47×10^{-3}	-2.78×10^{-3}
3.5	2.98	1.25×10^{-5}	1.29×10^{-5}	2.39	2.57×10^{-4}	-7.15×10^{-4}
4.0	3.24	1.21×10^{-8}	1.32×10^{-8}	2.39	5.08×10^{-6}	-3.47×10^{-5}
4.5	3.52	1.39×10^{-12}	1.74×10^{-12}	2.39	5.15×10^{-8}	-6.77×10^{-7}
5.0	3.82	1.43×10^{-17}	2.34×10^{-17}	2.39	2.72×10^{-10}	-6.07×10^{-9}

we have computed numerically with the aid of their energy eigenvalues, available in the literature (Hioe *et al* 1978). The results are shown in figures 3(*b*)-7(*b*) for $n=0$-4 respectively. The full curves are the exact wavefunctions $\Psi_n(x)$, while the dotted curves are the renormalised optimum $\Psi_n^{(0,1)}(x;\lambda_n(x))$. For the cases $n=0$ and 1 no dots are visible, for the curves coincide to within about the line width. For $n=2$, 3 and 4 the agreement is not so precise, but still respectable.

These linear axis plots cannot usefully depict the comparison of the exact and approximate wavefunctions in the large $|x|$ region where both are extremely close to zero. For this reason, we also include tables 1-5, which provide the numerical values of these wavefunctions on a coarse mesh of x values ranging from 0-5. In addition, we include in these tables the values of other approximate wavefunctions which are calculated by closely allied, albeit rather less sophisticated, methods. These entail the use of a fixed λ_n value for all x, namely that given in equation (3.9*b*), which follows from the optimisation of the first-order energy eigenvalue $E_n^{(0,1)}(\lambda)$, as described in

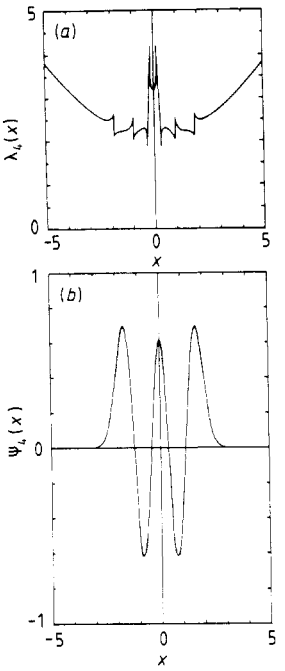

Figure 7. The same as figure 3 for the fourth excited state.

equations (3.8) and (3.9). One column of each table has the values of the zeroth-order wavefunction for this fixed $\lambda = \lambda_n$, i.e. $\Psi_n^{(0)}(x; \lambda_n)$, while another column has the values of the first-order wavefunction approximation (as renormalised) for this fixed λ_n, i.e. $\Psi_n^{(0,1)}(x; \lambda_n)$. A glance at the tables shows that these fixed λ_n approximate wavefunctions, especially the first-order one, can compete well with our renormalised $\Psi_n^{(0,1)}(x; \lambda_n(x))$ approximations at the smaller $|x|$ values. However, they fare very poorly for the larger $|x|$ values; the first-order perturbative fixed λ_n approximation appears to always develop an unphysical extra node there. This is not surprising, for the perturbative potential $V(\lambda)$ of equation (3.1*c*) becomes large with increasing $|x|$, causing a breakdown of orthodox perturbation theory, while our point-by-point optimised $\lambda_n(x)$ continues to yield reasonable results. It permits perturbation theory to function effectively even for strong couplings.

It is indeed the flexibility inherent in the point-by-point PMS wavefunction optimisation approach which makes this technique a welcome addition to the standard repertoire of approximation methods. We have seen here that its success for the quartic oscillator ground-state wavefunction may be extended to the excited states as well, once certain technical complications have been resolved.

References

Hioe F T, MacMillan D and Montroll E W 1978 *Phys. Rep.* **43C** 305
Kauffmann S K and Perez S M 1984 *J. Phys. A: Math. Gen.* **17** 2027
Stevenson P M 1981 *Phys. Rev.* D **23** 2916